Journal for
Electrochemistry and
Plating Technology

JEPT

Edited by: DGO-Fachausschuss Forschung – Hilden / Germany

Choline chloride-Ethylene glycol mixture as electrolyte for nano crystalline Nickel electrodeposits

Nickel plating was carried out in stable Nickel ion based deep eutectic solvent (DES). The DES electrolyte stability and possible structure were explained by using Fourier Transform Infrared spectroscopy (FTIR) and Temperature Modulated Differential Scanning Calorimetry (TMDSC) techniques. The conductivity and electrochemical studies for choline based eutectic solvents were analyzed by conductivity cell and electrochemical impedance spectroscopy respectively. Higher current efficiency, thickness and hardness of Nickel were obtained by Pulse current electrodeposition when compared with Direct current electrodeposition. Crystallographic orientation and structural morphology were studied by X-ray diffraction (XRD) and Atomic Force Microscopy (AFM) respectively. Coated Nickel plate's corrosion resistance and porosity...

Received: 2013-03-07
Received in revised form: 2013-05-27
Accepted: 2013-05-29

Keywords: Deep eutectic solvent, Nano crystalline thin film, Electrodeposition, Electrochemical impedance spectroscopy (EIS), Atomic force microscopy (AFM)

By R. Pavul Raj, J. Maharaja and S. Mohan

DOI: 10.12850/ISSN2196-0267.JEPT1972

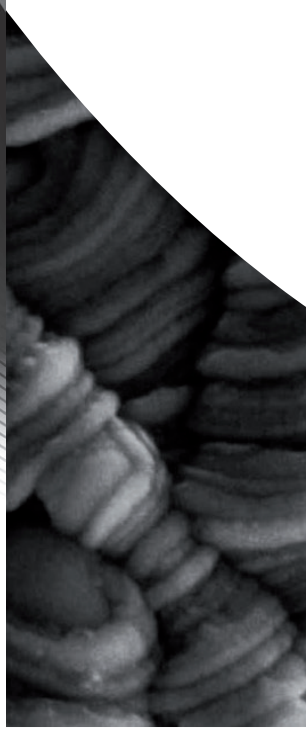

LEUZE VERLAG
seit 1902

Choline chloride-Ethylene glycol mixture as electrolyte for nano crystalline Nickel electrodeposits

*R. Pavulraj, J. Maharaja and S. Mohan**

** CSIR-Central Electrochemical Research Institute, Karaikudi – 630006, India*

Nickel plating was carried out in stable Nickel ion based deep eutectic solvent (DES). The DES electrolyte stability and possible structure were explained by using Fourier Transform Infrared spectroscopy (FTIR) and Temperature Modulated Differential Scanning Calorimetry (TMDSC) techniques. The conductivity and electrochemical studies for choline based eutectic solvents were analyzed by conductivity cell and electrochemical impedance spectroscopy respectively. Higher current efficiency, thickness and hardness of Nickel were obtained by Pulse current electrodeposition when compared with Direct current electrodeposition. Crystallographic orientation and structural morphology were studied by X-ray diffraction (XRD) and Atomic Force Microscopy (AFM) respectively. Coated Nickel plate's corrosion resistance and porosity properties were checked using potentiodynamic polarization and electrochemical impedance spectroscopy.

Keywords: Deep eutectic solvent, Nano crystalline thin film, Electrodeposition, Electrochemical impedance spectroscopy (EIS), Atomic force microscopy (AFM)

Paper: Received: 2013-03-07 / Received in revised form: 2013-05-27 / Accepted: 2013-05-29

DOI: 10.12850/ISSN2196-0267.JEPT1972

1. Introduction

Electrodeposition is a well-known field for corrosion resistance coatings, surface treatment technology and decorative type coatings. Improved surface finish, corrosion resistance and wear properties were achieved by electrodeposition of Nickel or Chromium [1-3]. Moreover Pulse electrodeposition has advantage than usual direct current electrodeposition. Pulse electrodeposition improved the mechanical and electrical properties of deposits [4]. In pulse plating three variables are important (on time, off time and current density). During Pulse on – time, high intense current densities and high negative overpotential was applied on the cathode surface. Due to the high overpotential the nucleation rate will get enhanced. At Pulse off – time, the equilibrium of cathodic concentration gradients will be formed by diffusion of metal ion from bulk concentration to cathode metal surface. Pulse plating leads to less porous surface, fine grained, increase in the wear resistance and reduction in the metal hydride formation [4-7]. Conventional aqueous solutions cannot be always used as electrolytes for dense coating because of limited potential window, hydrogen embrittlement and low thermal stability [8]. Similarly Deep eutectic solvent has an advantage over the aqueous solution like non-volatility, inflammability, low toxicity, good solubility, high thermal stability, wide electrochemical windows and high polarity [9-18]. The

deep eutectic solvent was the lowest complete melting point of mixture of components. In all other proportions, the mixture will not have a uniform melted system; some of the mixture will remain solid and some as liquid. In this paper, we deposited Nickel from choline chloride and ethylene glycol based deep eutectic solvent by using pulse current and direct current. The deposited Nickel film's corrosion properties and conductivity were studied. DES surface morphology and stability were also investigated in this paper.

2. Experimental section

The deep eutectic mixture was prepared as reported by Abbott et.al. [13]. In this electrolyte 8.4 g choline chloride ($HOC_2H_4N(CH_3)_3^+Cl^-$) (Acros > 99%), 28 ml ethylene glycol (Aldrich > 99%) 10 – 35 g $NiCl_2$ (Merck > 99%) and 0.5 g potassium chloride (Merck > 99%) were added and this mixture is stirred and heated to 70°C until a homogeneous, green color liquid is formed. For the Nickel deposition we used two electrode system. Insoluble high-density graphite was used as an anode. Mechanical buffing, degreasing, alkali electrocleaning and neutralization with acid pretreated copper sheets and mild steels were used as cathode, in both direct current and pulse current electrodeposition. Electrodeposition was carried out at ~45°C. For the electrochemical studies we used three electrode system. The Nickel deposited mild steel substrates were used for porosity calculation and impedance studies. Electrochemical Impedance Spectroscopy (EIS) was carried out in PARSTAT 2273 Princeton Applied Research with the power suite software. Impedance spectra were measured between the frequency ranges of 10 mHz to 100 kHz with 10 mV rms amplitude. One cm^2 substrate's surface area was used as working electrode, Ag / AgCl in saturated KCl was used as reference electrode and platinum foil was used as counter electrode.

3. Results and Discussion

3.1. Conductivity measurements

Conductivity was measured with Testronix 15 conductivity meter as a function of temperature (temperature was maintained with Julabo thermostat). Conductivities were studied by variation of Ni^{2+} ion concentration with 1:2 molar ratios of choline chloride and ethylene glycol (ethaline). *Figure 1a* shows the variation of conductivity for various Nickel concentrations as a function of temperature and TMDSC curve for the ethaline solution. Among the conductivity values 1:1 and 1:2 molar ratio of choline chloride, nickel (II) chloride mixture is having higher value. This is because of $NiCl_3^-$ formation act as driving force for hole formation to permit movement [8, 16]. Generally, the heavier anions leads to faster lattice defects and form a liquid easily. The mobility of Ni (II) ion in liquid form is high when compared to solid form. From *Figure 1a*, 1:1 ratio of Ethaline and $NiCl_2$ was deviating from linearity. It shows the instability of the ethaline solution [17]. In other molar ratio of Nickel ion variation, the concentration gradient of nickel content was higher and it reduces the conductivity of the electrolyte.

a

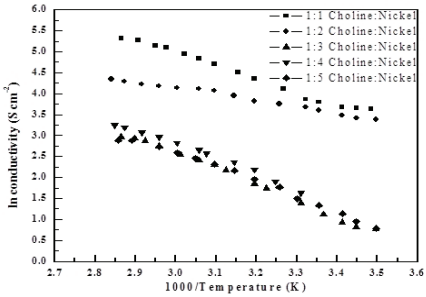

Fig. 1a: Comparison of conductivity of Ni(II) chloride dissolved in Ethaline complex

Choline chloride thermo properties were studied using METTLER TOLEDO TMDSC in the nitrogen

gas medium. Temperature Modulated Differential Scanning Calorimetry (TMDSC) calibrated with standard indium metal gave sharp endothermic melting point at 156°C. In *Figure 1b* we observed one sharp endothermic peak at 67°C and no peaks were seen at 0°C. At 67°C a sharp endothermic peak indicated phase transition of choline chloride with an integral area of peak as –1321 mJ and heat capacity (C*p*) value of –130 mJ K^{-1} g^{-1} as seen from *Figure 1b*. If any water molecule absorbs on choline chloride, it will appear as a peak on the water freezing point. Here the absence of water freezing point at 0°C indicated the absence of water moisture. Based on these experiments we concluded that no water content is persent in Choline chloride. Decomposition of choline chloride was obtained when the temperature is raised above the endothermic peak [18].

mation $NiCl_3^-$ along with $NiCl_2$.[8, 16, 18] Chloride ion was replacing one of the coordination sites in $NiCl_2$ from ethaline solution. The *Figure 2* FTIR spectrum, (Fourier Transform Infrared spectroscopy) gave stretching and bending frequency of the quaternary ammonium ion. The quaternary ammonium chloride ion-bending peak is obtained at 957 cm^{-1}. The intensity of 957 cm^{-1} peak diminished in both ethylene glycol and Ni(II) ion based deep eutectic mixture and this indicates chloride ion concentration is transferred to the solvent and form $NiCl_3^-$ ion. At 2360 cm^{-1} quaternary ammonium ion's stretching peak is also not observed in deep eutectic solvent (DES). This is due to the formation of the complex known as ethaline and $NiCl_3^-$ ion. [20, 21] 2000 cm^{-1} is stretching peak for ethylene glycol and chloride ion complex structure. The possible mechanism of ethaline

b

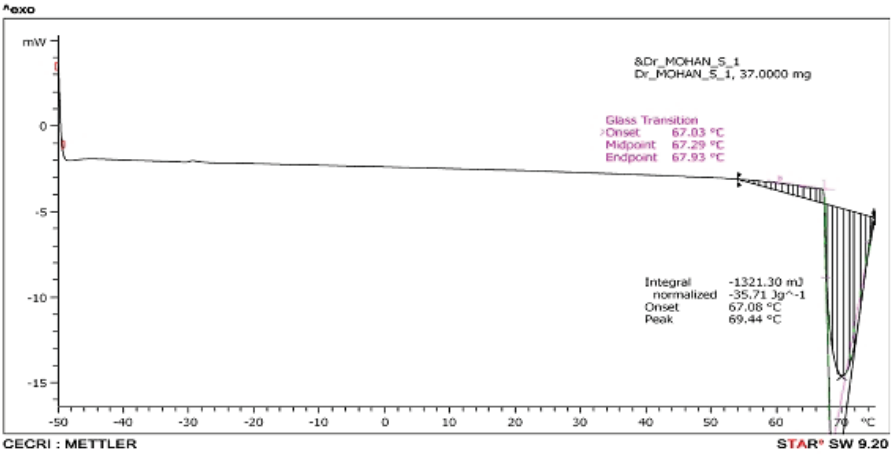

Fig. 1b: TMDSC spectrum of Choline chloride in nitrogen gas environment

3.2. FTIR studies

In deep eutectic solvent, chloride ion from choline chloride is drawn towards $NiCl_2$ for the formation and nickel complex formations were shown in *Figure 3*. Choline chloride complex with ethylene glycol to form ethaline. Then ethaline interact with metal salt to form an easily melt compound.

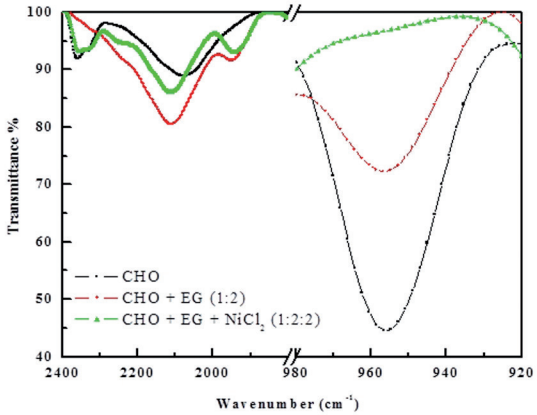

Fig. 2: Comparison of FTIR peaks of Choline and then Nickel complex

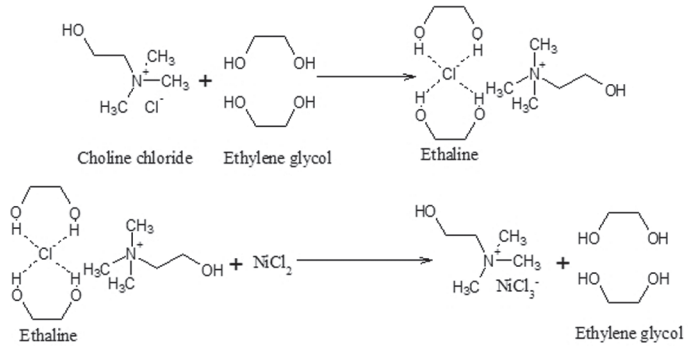

Fig. 3: Mechanism of $NiCl_3^-$ ion formation in ethaline based deep eutectic solvent

3.3. Electrochemical impedance studies

Observed impedance data were fitted and analyzed by ZSimpWin 3.22 software. The Bode plot diagrams (*Fig. 4*) were parabola shape but at low frequency region curve distracted slightly. It shows that mass transport also plays an important role. [22, 23] Reason behind is that diffusion process is also present in the equivalent circuit. At this point the element Q is defined as constant phase element (CPE) and given by the following equation.

$$Z_Q = (Y_Q (j\omega) ^{\alpha})^{-1} \quad [1]$$

Where ω is the angular frequency ($\omega = 2\pi f$), Y is admittance and the exponent α is non-linearity of the capacitor in electrode surfaces. If $\alpha = 1$, the Z_Q reduces to a capacitor C if $\alpha = 0$, it is considered as a simple resistor. The values at very high

frequencies give the solution resistance (R_s). The low frequency region gave the features of diffusion-control parameters. This fact allows us to calculate the diffusion control reaction of Ni(II) ionic species using the following equations.

$$R_s = R_{ct} + \sigma / \omega^{1/2} \quad [2]$$

$$\sigma = (RT / \sqrt{32}F^2A)\,[(1 / DO^{1/2}C_O^*) + (1 / D_R^{1/2}C_R^*)] \quad [3]$$

Here R, T, F, A, CO and C_R are gas constant, temperature, Faraday constant and surface area of working electrode bulk concentration of the oxidized and reduced species respectively. σ, D_O and D_R is specific conductance, diffusion coefficient of the oxidized and reduced species respectively. In *Figure 5* Z_{real} vs $\omega^{-1/2}$ gave a straight line for all five cases, (1:1, 1:2, 1:3, 2:1 and 3:1 ethaline and Ni (II) concentration respectively) and thus provide evidence for diffusion-controlled process [24]. Solution resistance varied by changing the concentration of the medium. The values of equivalent circuit elements were obtained by using the ZSimpWin 3.22 software. We measured solution resistance (Rs), double layer capacitance (C*dl*), charge transfer resistance (R*ct*), Diffusion parameters, Bare electrode surface capacitance (C*c*) and resistance (R*c*). These values are listed in *Table 1*. From the simulation value, solution resistance was lower for 1:1 (2.15 Ω) and 1:2 (4.92 Ω) Ethaline and Nickel solution. Conductivity is reciprocal of resistance. Similarly the double layer capacitance is low in 1:1 and 1:2 ratio of ethaline and Nickel ion solution. Diffusion based parameter, constant phase elements were same for all the cases. In electrodeposition, ethylene glycol contributes to smooth Nickel electrodeposition, it acts as a grain refiner [25, 26]. Nickel ion diffusion from ethaline based eutectic solvent is mainly contribute to constant phase element and similar behavior is reported by F. Golgovici et.al., work [27].

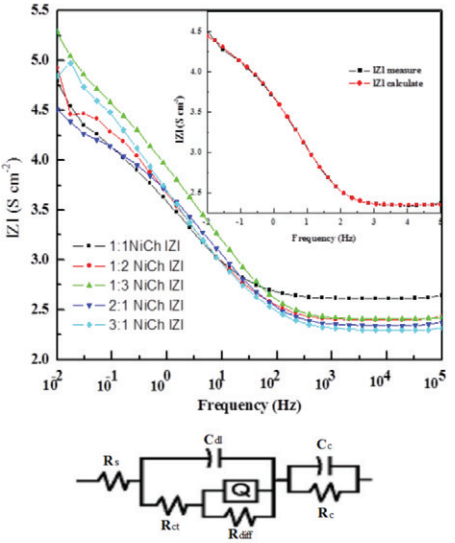

Fig. 4: Electrochemical impedance spectroscopy studies of Ni(II) chloride dissolved in ethaline eutectic solvent and schematic diagram of equivalent circuit

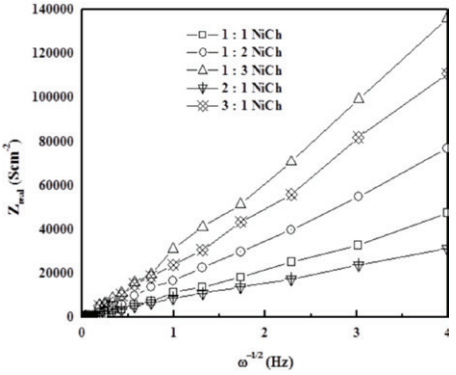

Fig. 5: Comparison of Z_{real} vs $\omega^{-1/2}$ for diffusion of Ni(II) ion from ethaline solution

3.4. DCD and PED methods for Nickel deposition

The cyclic voltammograms (*Fig. 6*) show the electrodeposition and dissolution of Ni on Pt wire

at ~45°C. Cyclic Voltammetry was carried out in PARSTAT 2273 Princeton Applied Research with the power suite software. The potential window is cycled between ± 1 V with respect to open circuit potential (OCP). Nickel deposition started nearly at - 600 mV vs Ag / Ag^+ reference cell but adsorption of nickel on Pt wire is initiated at - 200 mV. The inner figure shows the Choline chloride's electrochemical active potential window.

density in PED method. We got ~7 microns within 3 mins with 93.34% current efficiency in pulse electrodeposition. Hardness of coated nickel was measured in Everone hardness tester, DCD is having hardness 250–300 HV and in PED hardness is increased to 280–375 HV at 25 g load. Very thin pulsating diffusion thickness enhances the nucleation rate. Fine grained structure and less porous deposits were obtained in PED than that of DCD

Tab. 1: Comparison of the best fitting values of equivalent circuit elements from simulated impedance data in Choline based deep eutectic solvent

Ethaline : Nickel	Rs (ohm)	C (farad)	R (ohm)	Q ($S\text{-}sec^n$)	n (0<n<1)	R (ohm)	C (farad)	R (ohm)
1:1	0.0215	29.91 nF	410.9	68.84 F	0.7357	15.6 K	319.3 F	45.9 K
1:2	0.0492	49.06 nF	212.1	45.92 F	0.7432	13.47 K	435.5 F	16.01 K
1:3	201	6.67 F	284.4	40.04 F	0.7789	85.23 K	690.9 F	760.6 K
2:1	6.993	1.99 nF	119.8	52.5 F	0.7513	69.76 K	114.7 F	1.263 K
3:1	255.9	1.66 F	0.01	30.02 F	0.7411	417.9 K	93.92 F	145.8 K

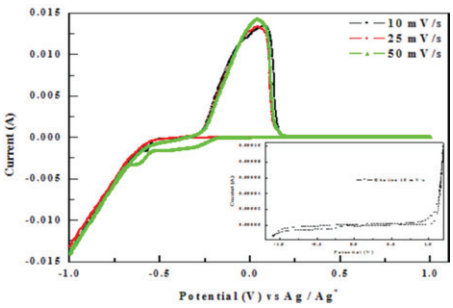

Fig. 6: Cyclic voltammograms on Pt (0.1 cm^2) for Ni(II) from ethaline based deep eutectic solvent

Bright nickel is deposited by both direct current (DCD) and pulse current electrodeposition (PED) in Ni based deep eutectic solvent as an electrolyte. Deposition time was 3 mins. In direct current electrodeposition maximum thickness of ~5 microns and 89.17% current efficiency were obtained at 0.2 mA cm^{-2}. The same current density 0.2 mA cm^{-2} was taken as average current and this is because of pulse peak current density is higher than direct current density and Desorption of adsorbed hydrogen take place at the cathode surface during each off-time (T_{Off}) [28].

3.5. X-ray diffraction

The deposited Nickel was characterized by X-ray diffraction PANalytical X'perPRO model, copper Kα (1.54Å) as a source for 2θ ranging from 10-90°. The X-ray diffraction spectra of nickel films were shown in *Figure 7*. The crystallite size of electrodeposited nickel was determined from FWHM of (111), (200) and (220) reflections according to the Debye-Scherrer equation [29]. The preferred crystalline orientation of the nickel films was evaluated by the relative texture coefficients RTC_{hkl} using equation 2.

$$RTC_{hkl}(\%) = (I_{hkl}/I^{\circ}_{hkl} \times 100) / (\sum I_{hkl}/I^{\circ}_{hkl}) \quad [4]$$

Where I_{hkl} are the relative intensities of the (hkl) lines measured in the diffractogram of the nickel films and I°_{hkl} are the corresponding intensities of a randomly oriented nickel film sample (JCPDS no.87-0712). The summation $\sum I_{hkl}$ was taken from the three lines visible in the diffraction spectra, i.e. (111), (200) and (220). The X-ray diffraction patterns of Ni films exhibit the pure FCC Ni in both DCD and PED conditions. The Bragg reflections corresponding to crystalline Ni were observed at 2θ = 44.63, 52.02, 76.62 for DCE and at 44.8, 52.01, 76.82 for PED method. In DCD texture coefficients are 51% for 111 plane, 24% for 200 and 220 plane. In PED, texture coefficients are 63% for 111 plane, 12% for 200 plane and 24% for 220 plane. Calculated PED Ni is having a very small crystalline size of 23 nm, which is smaller than the Ni obtained by DCD (37 nm) techniques. In pulse plating small crystalline size and dense coating was observed. But in the direct current method the continuous diffusion and migration of nickel ion was not fully understandable in DES. Crystal phase orientation was changed in the direct current method.

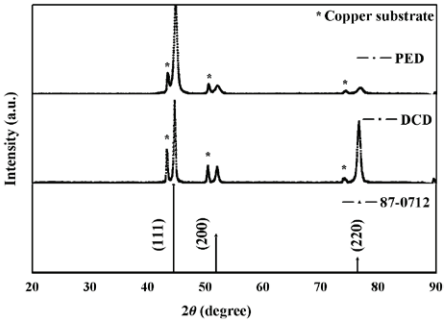

Fig. 7: XRD curves of the electrodeposited Nickel in direct current method (DC current 0.2 mA/cm^2 and Time 180 seconds) and pulse method (average current 0.2 mA, Duty cycle 10, peak current 2 mA, duration time 180 seconds)

3.6. Atomic Force Microscopy studies

Structural morphology (AFM image) of electrodeposited Nickel under DCD and PED conditions

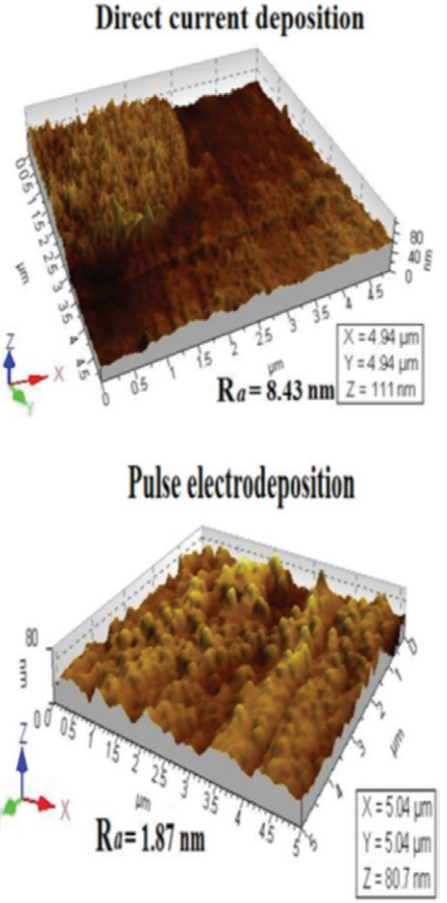

Fig. 8: Atomic Force Microscopy image of deposited Nickel in direct current method (DC current 0.2 mA/cm^2 and Time 180 seconds) and pulse method (average current 0.2 mA, Duty cycle 20, peak current 2 mA, duration time 180 seconds)

was characterized using Picoscan 2000 in contact mode. *Figure 8* shows an AFM image of deposit nickel in direct current density of 0.2mA cm^{-2},

time 180 seconds, its approximate average grain size is 200-300nm and AFM image of deposited nickel in pulse method is having approximate average grain size of 100-250nm when average current density of 0.2mA cm^{-2} is used. The duty cycle is 20 and time of deposition is 180 seconds. Both DCD and PED method have fine nano crystalline sized nickel deposits with less mean deviation of roughness. (R_a) Needles type surface morphology was observed in direct current method but some regular type of surface morphology was observed in pulse plating.

3.7. Corrosion resistance studies with potentiodynamic polarization

Figure 9a shows potentiodynamic polarization curves for electrodeposited nickel in 3.5% NaCl solution. All the studies were done between ± 0.25V vs OCP. From this figure we observe that

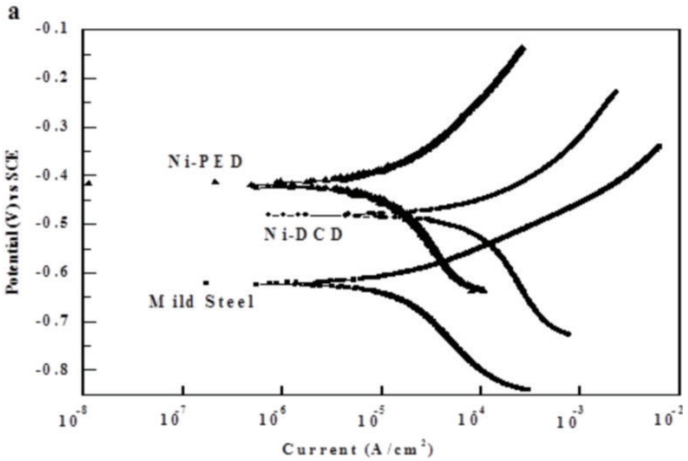

Fig. 9a: Comparison of Tafel curves of deposited nickel on steel in 3.5 M NaCl solution

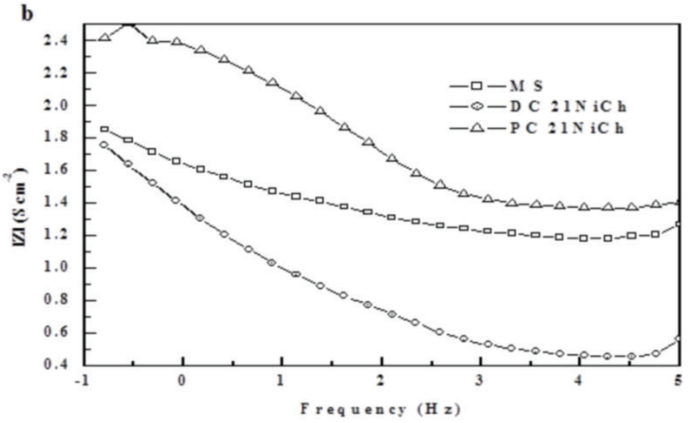

Fig. 9b: Electrochemical Impedance Spectroscopy of deposited Nickel on MS

the activation polarization resistance potential is shifted towards the noble potential region from cathodic region. The corrosion current density (I_{corr}) and corrosion potential (E_{corr}) were calculated from the intercept of the Tafel slopes. The corrosion rate in mills per year was estimated from the polarization curves, and the values are given in *Table 2*. Among all the samples Ni-PED / MS exhibits lower values of E_{corr} and corrosion rate than that of samples Ni-DCD / MS and mild steel (MS). From these Ni-PED / MS exhibits the best corrosion resistance, and this is due to the dense nanostructure coating. Ni (220) surface was high in DCD method deposited nickel when compared with the standard PED method. The result of Ni (220) plane intensity reduced the hydrogen evolution by means of low I_{corr} of DCD method electrodeposition [30].

Tab. 2: Comparison of corrosion parameters of deposited nickel on mild steel in 3.5M NaCl corrosion medium

Sample	OCP (mV)	E_{corr} (mV)	I_{corr} (μA)	Corrosion rate (mpy)	R_{ct} Ω cm^2	C_{dl} μF cm^2	Porosity %
Mild steel	-486	-623	20.61	10.44	40	1115	---
DCD (0.2mA)	-381	-481	183	8.84	330	822	0.0790
PED (0.2mA)	-351	-418	20.84	7.78	2881	613	0.0090

3.8. Corrosion resistance studies with electrochemical impedance spectra tests

We measured impedance spectra for the electrodeposited Nickel substrate in 3.5% NaCl aqueous solution and the results are given in *Figure 9b*. Impedance spectra were measured between the frequency ranges of 100 mHz to 100 kHz with 10 mV rms scan rate. The corrosion resistance (R_{ct}) of PED Nickel is greater than mild steel and DCE Nickel samples. The increased R_{ct} values and decreased C_{dl} values for Ni deposits clearly confirm the better corrosion resistance of these PED and DC deposit compared with bare mild-steel substrates, because of the better properties of deposit, less roughness and the Nickel dissolution is less. Stimulated fitting circuit is similar to that used in our previous work [31].

3.9. Porosity of Ni-DCD and Ni-PED systems

It is possible to determine the porosity of a coating using an electrochemical measurement technique that determines the ratio of the current density through the pores and the coating [32]. Elsener et.al., estimated the porosity of TiN coated mild steel from the shift of the corrosion potential caused by the presence of the coating (ΔE_{corr}) and from the individual polarization resistance of the coatings (R_p) and the substrate materials ($R_{p,s}$) as given in equation 3 [31, 33].

$$P = (R_{p,s} / R_p) * 10^{-|\Delta Ecorr| / ba} \quad [5]$$

Where b_a is the Tafel slope of the active dissolution of mild steel. Using this equation, and the values of $R_{p,s}$ = 26 Ω cm^2 and b_a = 0.171 V decade^{-1} determined from separate measurement on an uncoated mild steel (MS) substrate in 3.5% NaCl solution, we estimated the porosity of the Ni-(PED) has 0.24% and Ni-(DCD) is 1.48%. From this value the PED nickel coating system is having ten times lower porosity than the DCD nickel system.

4. Conclusion

Stable choline chloride based deep eutectic solvent for electrodeposition of Nickel was pre-

pared. Conductivity of different concentration of ethaline with Nickel ion were measured and among the conductivity values the 1:2 molar ratio holds good for deposition of Nickel. Structure and stability of Nickel ion in deep eutectic solvent were analyzed by using TMDSC and FTIR spectroscopy. 1:2 ratio of Ethaline and Nickel ion had lower charge transfer resistance and higher double layer capacitance. Ethylene glycol from the deep eutectic mixture contributed to formation of smooth nano Nickel electrodeposition and double layer capacitance. Deposited nickel by PED method having less roughness, 9 times higher R_{ct} and lower corrosion rate values than that of DCD Nickel.

5. Acknowledment

Authors thank the Department of Science and Technology New Delhi for a research grant under SERC (Engineering Sciences) scheme no. SR/S3/M/0030/2009. We thank the Director, (CSIR-CECRI) to carry out the research work.

Reference

[1] C.K. Chung; W.T. Chang; C.F. Chen; M.W. Liao, *Mater.lett.* 65, 416 (2011)

[2] N. Imaz; E. Garcia-Lecina; J. A. Diez, *T.I.Met.Finish.* 88, 256 (2010)

[3] Y. Boonyongmanreerat; S. Saenapitak; K. Saengkiettiyut, *J.Alloy.Compd.* 487, 479 (2009)

[4] J.C. Puippe; F. Leaman, *Theory and Practice of Pulse Plating*, AESF: Orlando, Florida (1986)

[5] S. Mohan et.al., *Trans.Inst.Met.Fin,* 81(5), 1 (2003)

[6] A. Lahiri; Rupakdas, *J.Appl.Electrochem.* 40, 1991 (2010)

[7] Lin, C.C; Huang, C.M, *JCT Res.* 3, 99 (2006)

[8] Frank Endres; Douglas MacFarlane; Andrew P. Abbott, *Electrodeposition form ionic liquids*, WILEY-VCH Verlag GmbH & Co.: KGaA, Weinheim (2008)

[9] A. Florea; L. Anicai; S. Costovici; F. Golgovici; T. Visan, Surf. InterfaceAnal. 42, 1271 (2010)

[10] W. Simka; D. Puszczyk; G. Nawrat, *Electrochim.Acta* 54, 5307 (2009)

[11] P. Wasserscheid; T. Welton, *Ionic liquids in synthesis*, WILEY-VCH Verlag GmbH & Co.: KgaA, Weinheim (2003)

[12] F. Endres; S.Z. Abedinw, *Phys.Chem.Chem.Phys.* 8, 2101 (2006)

[13] A.P. Abbott; G. Capper; S. Gray, *Chem.Phys.Chem.* 7, 803 (2006)

[14] A.P. Abbott; R.C. Harris; K.S. Ryder, *J.Phys.Chem.B* 111, 4910 (2007)

[15] Xu,W; Copper,E.I; Angell,C.A, *J.Phys.Chem.B* 107, 6170 (2003)

[16] A.P. Abbott; G. Capper; D.L. Davies; R.K. Rasheed; V. Tambyrajah, *Chem.Commun.* 1, 70 (2003)

[17] Kurt Haerens; Edward Matthijs; Koen Binnemans; Bart Van der Bruggen, *Green Chem.*, 2009, **11**, 1357–1365

[18] E.P. Grishina; A.M. Pimenova; L.M. Ramenskaya, *Russ.J.Electrochem.* 45, 938 (2009)

[19] K.R. Seddon; A. Stark; M. Torres, *Pure.Appl.Chem.* 72, 2275 (2000)

[20] K. Fujii; T. Nonaka; Yu Akimoto; Y. Umebayashi; S. Ishiguro, *Anal.Sci.* 24, 1377 (2008)

[21] A. Samanta, *J.Phys.Chem.Lett.* 1, 1557 (2010)

[22] http://chemistry.tkk.fi/en/research/physical/projects/ionic_liquids/

[23] Y.V. Ingelgem; E. Tourwe; J. Vereecken; A. Hubin, *Electrochi. Acta* 53, 7523 (2008)

[24] B. Rosborg; J. Pan, *Electrochi. Acta* 53, 7556 (2008)

[25] A.J. Bard; L.R. Faulkner, *Electrochemical methods 2nd Edition,* John Wiley & Sons, Inc., U.K. (2004)

[26] T. Chowdhury; D.P. Casey; J.F. Rohan, *Electrochem Commun,* 11, 1203 (2009)

[27] L.E.Moron; T.Meas; R.O. Borges; J.J. Bueno; R.G.Trejo, *Int.J.Electrochem.Sci.,* 4, 1735 (2009)

[28] F. Golgovici; A. Cojocaru; M.Nedelcu; T. Visan, *Chalcogenide Letters* 6, 323 (2009)

[29] H.P. Klug; L.E. Alexander, *X-ray diffraction procedures, 2ed.*, John Wiley & Sons, New York (1974)

[30] Zaki Ahmad, *Principles of Corrosion Engineering and Corrosion Control,* Elsevier Science & Technology Books (2006)

[31] G. Saravanan; S. Mohan, *J.Appl.Electrochem.* 39, 1393 (2009)

[32] Tato W; Landolt D, *J.Electrochem.Soc.* 145, 4173 (1998)

[33] Elsener B; Rota A; Bohni H, *Mater.Sci.forum*. 44, 29 (1989)

Rayappan Pavul Raj
Electroplating and Metal Finishing Technology Division,
CECRI - Central Electrochemical Research Institute,
Karaikudi – 630006, Tamilnadu, India

J. Maharaja
Electroplating and Metal Finishing Technology Division,
CECRI - Central Electrochemical Research Institute,
Karaikudi – 630006, Tamilnadu, India

Dr. S. Mohan
Head of the division
Electroplating and Metal Finishing Technology Division,
CECRI - Central Electrochemical Research Institute,
Karaikudi – 630006, Tamilnadu, India

CONTACT:

EUGEN G. LEUZE VERLAG KG
Ralf Schattmaier
Karlstraße 4
88348 Bad Saulgau
Germany

Email: ralf.schattmaier@leuze-verlag.de
Phone: +49 0 7581 4801-12
Fax: +49 0 7581 4801-10